Polymer Vol. 37 No. 9, pp. 1663–1667, 1996

0032-3861/96/$15.00+0.00

Ab initio calculation of ethylene insertion in zirconocene catalyst systems: a comparative study between bridged and unbridged complexes

V. L. Cruz*, A. Muñoz-Escalona† and J. Martinez-Salazar‡§
**Centro Tecnico de Informatica, CSIC, Pinar 19, 28006 Madrid, Spain*
†Repsol I + DT, Embajadores 183, 28045 Madrid, Spain
‡Instituto de Estructura de la Materia, CSIC, Serrano 1919, 28006 Madrid, Spain
(Received 3 August 1995)

The *ab initio* method at the Hartree–Fock level has been used on two zirconocene systems, the unbridged $Cp_2ZrCH_3^+$ and the bridged $(Si(CH_3)_2)Cp_2ZrCH_3^+$ compounds. For each complex the insertion of an ethylene molecule has been followed from reactant to product through the corresponding transition states. The calculated activation energies are of the order of magnitude of those obtained experimentally, explaining the higher activity found for the unbridged catalytic complex compared to the bridged. The geometries are in agreement with other studies and comparable with those derived by crystallographic methods. The α-agostic interaction observed in the reactants as well as in the transition states and resulting products confirms that the Brookhart–Green mechanism is followed for the polymerization reaction. Copyright © 1996 Elsevier Science Ltd.

(Keywords: organometallic complexes; zirconocene catalysts; ethylene)

INTRODUCTION

Ziegler–Natta (ZN) and metallocene catalysts comprise an important class of organometallic compounds that are widely used in the polymerization of olefins[1–3]. The most widely accepted mechanisms for ZN polymerization are those proposed by Cossee and Arlman[4] and by Brookhart and Green[5].

Quantum-mechanical methods can provide important insight concerning the mechanistic details of the catalytic processes. Olefin polymerization by using ZN and metallocene catalyst systems has been studied theoretically by a number of authors[6–9]. Most of the publications are concerned with the prediction of the structural stereoselectivity of these catalysts using molecular mechanics calculations[10–12]. However, it is much more difficult to predict experimental activities for ethylene polymerization by using quantum-mechanics methods[6,8]. These studies have been primarily concerned with the initial step in the polymerization process, involving the insertion of an ethylene monomer between the methyl ligand and the active transition metal.

It has been proposed that in the metallocene catalyst the active centre is a cationic species formed by removing one of the two methyl ligands by means of the co-catalyst[13,14]. These systems are basically composed of Ti, Zr and Hf transition-metal centres bearing ligands that could be considered as not directly involved in the reaction and usually a methyl ligand, which forms the active carbon–metal bond. The ligands attached to the transition metal can influence the catalytic activity by electronic and steric effects. Also subjected to study are molecules containing a bridge group between the inactive ligands[8].

In the present work a comparison between both bridged and unbridged zirconocene systems is provided relative to the primary olefin insertion process. A similar study was previously published by others where a zirconocene containing a $-SiH_2-$ bridge was considered along with the unbridged structure[9]. They found no significant difference between both systems, neither geometrical nor energetic. We performed, however, *ab initio* calculations at different levels of theory to search for differences in the catalytic behaviour and compare with the experimental results. In this case the bridge consisted on a dimethyl silane fragment $-Si(CH_3)_2-$.

COMPUTATIONAL METHODS

The initial structures for the catalyst were modelled after the geometries derived from similar compounds found in the Cambridge Crystallographic Database[15]. Molecules were selected to contain two Cl atoms as ligands in the active site where the reaction is going to take place.

One Cl atom was substituted by a methyl ($-CH_3$) group and the other Cl was removed and an ethylene molecule (C_2H_4) was placed at the active complex.

---

§ To whom correspondence should be addressed

This structure is then subjected to geometry optimization within the Hartree–Fock model with the STO-3G (Slater-type orbitals, three Gaussian) minimal basis set using the Gaussian 92 package[16]. The structure of the product resulting from the ethylene insertion (propyl fragment formation) was also obtained by geometry optimization.

The transition-state geometry was found by applying the linear synchronous transit algorithm[17] to locate a maximum in the path from reactant to product. This structure is subsequently minimized to the true transition state of the appropriate curvature within the specified model.

Frequency calculations were then performed to ensure that the stationary points found correspond to local minima for the initial reactant and final product as well as for the transition state.

Single-point calculations were performed on the mentioned reactants and transition states using higher levels of theory to see its effect on the activation barrier for the insertion reaction. To this end, two models incorporating electron correlation were considered: on the one hand, the MP2 perturbational correction[18]; on the other hand, the density-functional theory method incorporating non-local extensions, as parametrized by Becke[19] for the exchange terms and by Lee *et al.*[20] for the correlation terms. The basis set used along with these models consisted of 3-21G quality for atoms corresponding to the ligands, and the 3-21G** set for those atoms more directly involved in the reaction. The pseudopotential known as LANL2DZ[21–23] and associated basis set was used for the central Zr atom.

RESULTS

Geometries

The optimized structures for reactant, transition state and product are shown respectively in *Figure 1* for the unbridged system and in *Figure 2* for the bridged zirconocene. The geometrical parameters for the active site obtained for the mentioned structures with the HF/STO-3G model are tabulated in *Table 1*.

The main differences observed between the bridged

Table 1 Geometrical parameters for the active site (distances are in Å and angles in degrees)

		Unbridged	CH_3–Si–CH_3
Angle C2–Zr–C1	Reactant	73.61	75.96
	Transition state	52.43	52.54
	Product	29.77	29.97
Distance Zr–H1a	Reactant	2.87	2.87
	Transition state	2.36	2.33
	Product	2.29	2.32
Distance Zr–C1	Reactant	2.30	2.39
	Transition state	2.30	2.30
	Product	2.94	2.91
Distance Zr–C2	Reactant	2.78	2.73
	Transition state	2.64	2.64
	Product	3.09	3.08
Angle C3–C2–Zr	Reactant	75.17	76.28
	Transition state	62.91	63.09
	Product	45.27	45.76

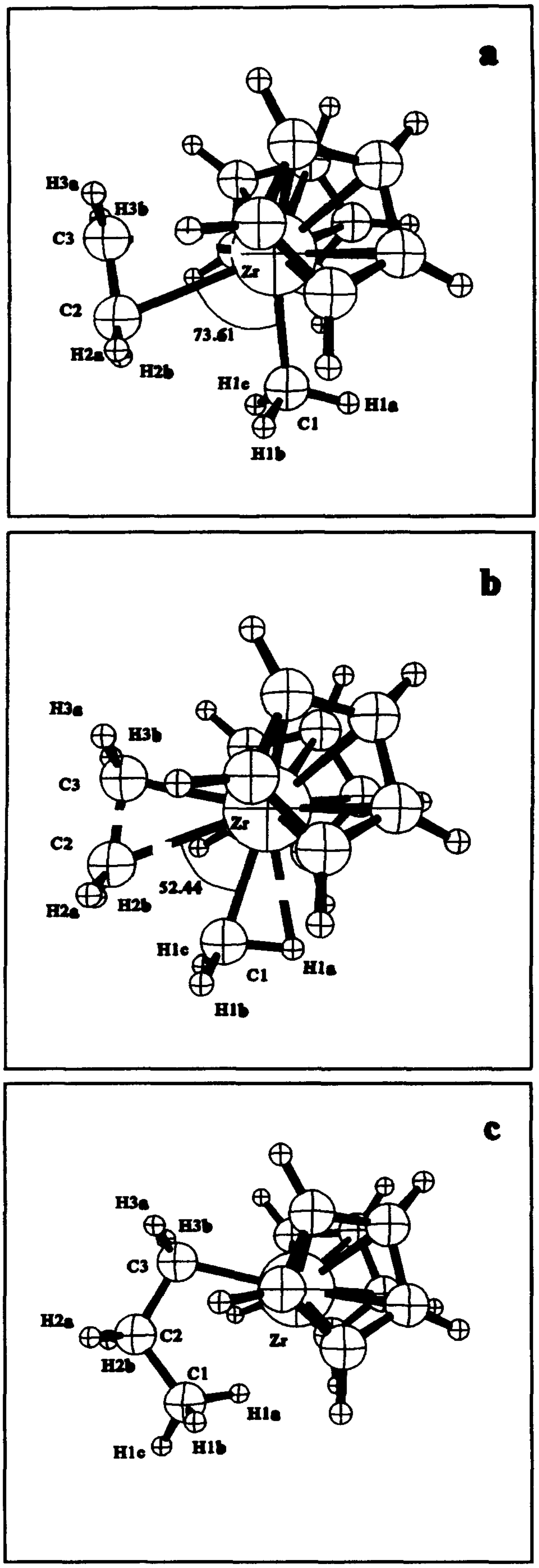

Figure 1 Optimized structures for the unbridged zirconocene complex: (a) reactants, (b) transition state and (c) resulting product after ethylene insertion

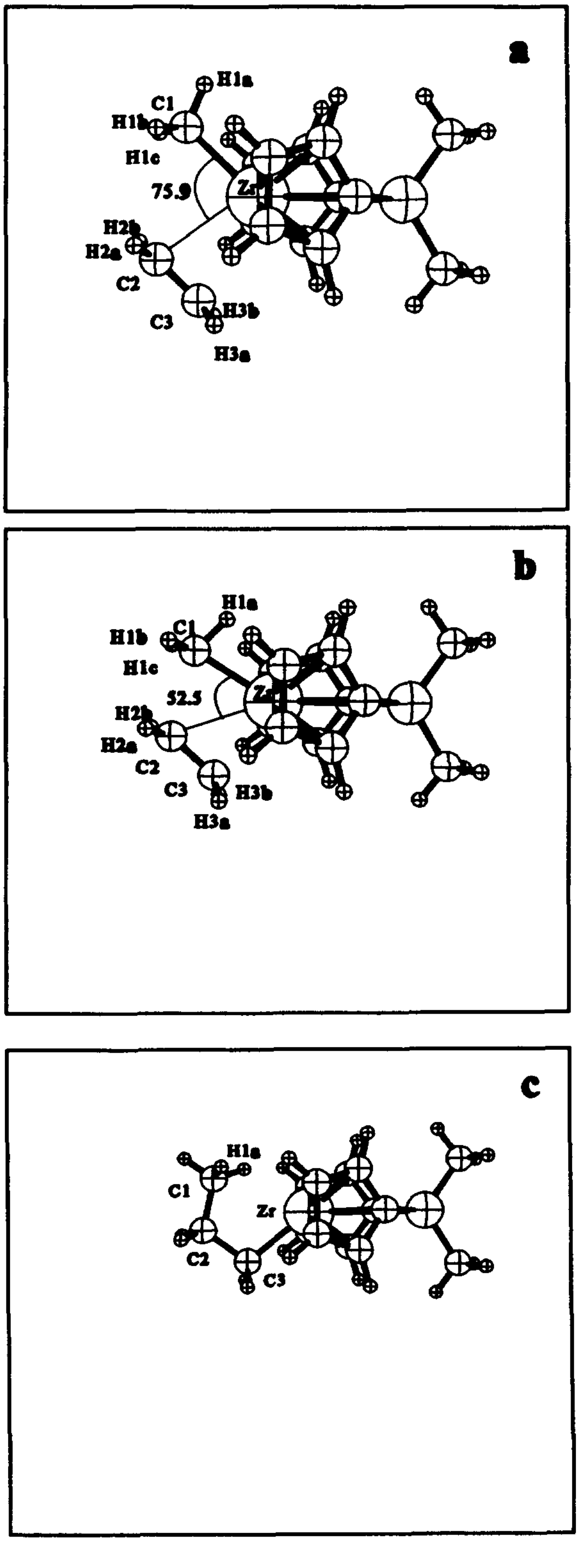

Figure 2 Optimized structures for the bridged zirconocene complex: (a) reactants, (b) transition state and (c) resulting product after ethylene insertion

and unbridged catalyst reside in the π-complex of the reactant. For instance, the angle difference between Zr–CH_3 and $CH_2{=}CH_2$ bonds is as much as 2.4° (73.61° vs. 75.96°; see *Table 1* and *Figures 1* and *2*). This tendency is also experimentally confirmed with crystallographic data on compounds with Cl atoms as ligands at the active site positions (even with Ti as central transition metal)[24–27].

The bonding distances Zr–C1 and Zr–C2 are slightly smaller for the bridged catalyst (2.31 Å vs. 2.29 Å for the Zr–C1 distance and 2.787 Å vs. 2.732 Å for the Zr–C2 distance in *Table 1*). However, the Zr–H1a distance remains almost equivalent in both cases. There is also a slight increase in the angle formed by the Zr and the two ethylene atoms in the bridged system (75.17° vs. 76.28° in *Table 1*).

In the transition state the differences between the bridged and unbridged catalyst are less remarkable. The angle C2–Zr–C1 is slightly greater for the bridged compound than for the unbridged (52.54° vs. 52.44°; see *Table 1* and *Figures 1* and *2*). The similarity in the remaining geometrical parameters suggests that both transition structures are almost equivalent.

For the products the differences between bridged and unbridged are approximately the same as for the transition state (see *Table 1*).

Energies

The activation energies calculated as the difference between transition-state and reactant energies are $11.3\,\mathrm{kcal\,mol^{-1}}$ for the unbridged and $12.8\,\mathrm{kcal\,mol^{-1}}$ for the bridged compound at the HF/STO-3G level.

These magnitudes differ tremendously when considering improved models and single-point calculations on the found stationary points with both the density-functional treatment (DFT) and Moller–Plesset perturbation model (MP2). In fact the activation barrier is lowered to $6.6\,\mathrm{kcal\,mol^{-1}}$ for the unbridged compound using both DFT and MP2 calculations. However, for the bridged system the activation barrier even disappears regardless of the calculation method. Similar results have been observed with titanocene $Cp_2Ti{-}CH_3^+$ catalyst using *ab initio* calculations[6].

Charge distribution

Taking into account the Mulliken population analysis[28], atomic charges condensed to atoms are tabulated for the unbridged and bridged catalyst (*Table 2*). Contrary to what was observed for the geometrical parameters, the charge distribution differences between the atoms of the bridged and unbridged catalysts are very small (see *Table 2*), indicating that the introduction of the $-Si(CH_3)_2-$ bridge has little influence on the charge of the central metal atom[29]. When reactants or transition states are considered, there is a slight reduction in positive charge on the Zr atom in the bridged zirconocene. This could slightly influence the difference of the interaction between the positively charged Zr with the ethylene monomer in the bridged and unbridged catalysts. Thus, when looking at the Mulliken matrix condensed to atoms one can get some picture of the atom–atom interactions strength. *Table 3* reproduces an extract of the Mulliken matrix corresponding to heavy atoms in the active site respectively for the unbridged and bridged reactants. It is interesting to note that the interaction between the Zr and both ethylene carbons is stronger in the unbridged compound (0.07 for Zr–C2 and 0.08 for Zr–C3 in *Table 3*) compared to the bridged complex (0.06 for Zr–C2 and 0.07 for Zr–C3 in *Table 3*). These facts could also explain the superior reactivity found for the unbridged zirconocene.

Table 2 Mulliken charges for atoms in the active site for both compounds

	Reactant		Transition state		Product	
	Unbridged	Bridged	Unbridged	Bridged	Unbridged	Bridged
Zr	0.49	0.47	0.46	0.44	0.58	0.58
C1	−0.28	−0.29	−0.28	−0.28	−0.18	−0.18
H1a	0.05	0.03	0.06	0.05	0.00	0.01
H1b	0.04	0.03	0.07	0.07	0.10	0.11
H1c	0.04	0.05	0.07	0.07	0.07	0.07
C2	−0.08	−0.09	0.01	0.01	−0.10	−0.10
H2a	0.13	0.13	0.13	0.13	0.07	0.07
H2b	0.12	0.13	0.13	0.13	0.07	0.07
C3	−0.13	−0.12	−0.20	−0.20	−0.21	−0.21
H3a	0.12	0.12	0.09	0.09	0.04	0.04
H3b	0.11	0.12	0.09	0.09	0.05	0.04

Table 3 Mulliken matrix elements condensed to atoms in the active π-complex

Atom pair	Unbridged	Bridged
Zr–C1	0.34	0.33
Zr–C2	0.07	0.06
Zr–C3	0.08	0.07
C2–C3	0.54	0.55

DISCUSSION

The geometries obtained for the catalyst systems are in close agreement with the crystallographic structures for the non-participating fragments in the insertion process[24–27]. Furthermore, the structures obtained for the different stationary points compare well with related studies of unbridged[9] and bridged[8] catalyst systems. The main difference between the optimized structures in both zirconocenes is the angle formed by the methyl C1 atom, the Zr atom and the ethylene C2 atom in the reactants. The angle increase observed for the bridged structure might be associated with a decrease in the Cp–Zr–Cp angle due to the presence of the $-Si(CH_3)_2-$ group.

The activation energies obtained at the HF/STO-3G level are more in agreement with the experimental findings[30] in the sense that they reflect the correct order: the unbridged system is more active than the bridged. This order is inverted when considering electron correlation through either Moller–Plesset or density-functional theory. This refers to the single-point calculations on stationary points found at the HF level. It is noticeable that no activation barrier is found for the bridged compound. Although this result is similar to those reported by Weiss and coworkers[6], it might indicate that further optimization at a correlated level should be done.

The agostic interaction observed in the reactants as well as in the transition structures and in the products confirms that the Brookhart–Green mechanism[4] is followed instead of the mechanism proposed by Cossee and Arlman[5].

The activation energy for the bridged compound is higher compared to the unbridged complex, in agreement with observed experimental polymerization activities[31].

Another interesting observation is a longer bond distance between the Zr and the CH_3 ligand for the unbridged zirconocene along with a weaker C2–C3 interaction in the ethylene monomer observed in this compound compared to the situation in the bridged complex. These facts could provide a geometrical and electronic interpretation to the smaller activation barrier for the insertion step obtained for the unbridged catalytic system. However, as can be seen in *Table 3* the Zr–CH_3 interaction in the unbridged is stronger compared to the bridged complex, which is the opposite to the order of activity found.

The discrepancy in the electronic results could indicate that the geometrical factors take a preponderant role over the electronic considerations in the explanation of the energetic differences.

The HF/STO-3G model is known to present several deficiencies arising from the rigidity of the basis function and the lack of electron correlation. In spite of these disadvantageous characteristics, the model still provides an inexpensive way of doing *ab initio* calculations on systems with more than a few atoms. Energy calculations and geometry optimizations can be used as starting points in higher-level calculations, saving considerable computational resources. An appropriate knowledge of initial structure and Hessian is essential to successfully reach the correct stationary points in an optimization[32].

For comparison purposes even some useful results can be extracted from these calculations and problematic steps can be devised before running more complete calculations.

ACKNOWLEDGEMENTS

Thanks are due to the CICYT (Grant MAT94-0825) for the support of this investigation.

REFERENCES

1 Boor, J. 'Ziegler–Natta Catalysts and Polymerizations', Academic Press, New York, 1979, p. 1

2 Sinn, H. and Kaminsky, W. *Adv. Organomet Chem.* 1980, **18,** 99

3 Tait, P. J. T. 'Transition Metal and Organometallics as Catalysts

for Olefin Polymerization' (Eds. W. Kaminsky and H. Sinn), Springer, Berlin, 1988, p. 315
4 Arlman, E. J. and Cossee, P. *J. Catal.* 1964, **3,** 99
5 Brookhart, M. and Green, M. L. H. *J. Organomet. Chem.* 1983, **250,** 395
6 Weiss, H., Ehrig, M. and Ahlrichs, R. *J. Am. Chem. Soc.* 1994, **116,** 4919
7 Castonguay, L. A. and Rappe, A. K. *J. Am. Chem. Soc.* 1992, **114,** 5832
8 Yoshida, T., Koga, N. and Morokuma, K. *Organometallics* 1995, **14,** 746
9 Woo, T. K., Fan, L. and Ziegler, T. *Organometallics* 1993, **13,** 432
10 Yu, Z. and Chien, J. C. W. *J. Polym. Sci. (A) Polym. Chem. Edn.* 1995, **33,** 125
11 Yu, Z. and Chien, J. C. W. *J. Polym. Sci. (A) Polym. Chem. Edn.* 1995, **33,** 1085
12 Kawamura-Kuribayashi, H., Koga, N. and Morokuma, K. *J. Am. Chem. Soc.* 1992, **114,** 8687
13 Dyachkovskii, F. S., Shilov, A. K. and Shilov, A. E. *J. Polym. Sci. (C)* 1967, **16,** 2333
14 Jordan, R. F., Bajgur, C. S., Willet, R. and Scott, B. *J. Am. Chem. Soc.* 1986, **108,** 7410
15 Allen, F. H., Davies, J. E., Galloy, J. J., Johnson, O., Kennard, O., Macrae, C. F., Mitchell, E. M., Mitchell, G. F., Smith, J. M. and Watson, D. G. *J. Chem. Info. Comput. Sci.* 1991, **31,** 187
16 Frisch, M. J., Trucks, G. W., Schlegel, H. B., Gill, P. M. W., Johnson, B. G., Wong, M. W., Foresman, J. B., Robb, M. A., Head-Gordon, M., Replogle, E. S., Gomperts, R., Andres, J. L., Raghavachari, K., Binkley, J. S., Gonzalez, C., Martin, R. L., Fox, D. J., Defrees, D. J., Baker, J., Stewart, J. J. P. and Pople, J. A. 'Gaussian 92/DFT', Revision G.3, Gaussian Inc., Pittsburgh, PA, 1993
17 Halgren, T. A. and Lipscomb, W. N. *Chem. Phys. Lett.* 1977, **49,** 225
18 Moller, C. and Plesset, M. S. *Phys. Rev.* 1934, **46,** 618
19 Becke, A. D. *Phys. Rev. (A)* 1988, **38,** 3098
20 Lee, C., Yang, W. and Parr, R. G. *Theochem* 1987, **163,** 305
21 Hay, P. J. and Wadt, W. R. *J. Chem. Phys.* 1985, **82,** 270
22 Wadt, W. R. and Hay, P. J. *J. Chem. Phys.* 1985, **82,** 284
23 Hay, P. J. and Wadt, W. R. *J. Chem. Phys.* 1985, **82,** 299
24 Soloveichik, G. L., Arkhireeva, T. M., Bel'skii, V. K. and Bulychev, B. M. *Metalloorg. Khim. (Organomet. Chem. USSR)* 1988, **1,** 226
25 Bajgur, C. S., Tikkanen, W. R. and Petersen, J. L. *Inorg. Chem.* 1985, **24,** 2539
26 Clearfield, A., Warner, D. K., Saldarriaga-Molina, C. H., Ropal, R. and Bernal, I. *Can. J. Chem.* 1975, **53,** 1622
27 Bajgur, C. S., Tikkanen, W. R. and Petersen, J. L. *Inorg. Chem.* 1985, **24,** 2539
28 Mulliken, R. S. *J. Chem. Phys.* 1955, **23,** 1833
29 Woo, T. K., Fan, L. and Ziegler, T. *Organometallics* 1993, **13,** 2252
30 Muñoz-Escalona, A. and Parada, A. *Polymer* 1979, **20,** 474
31 Karol, F. J. and Kao, S. C. *New J. Chem.* 1994, **18,** 97
32 Schlegel, H. B. 'New Theoretical Concepts for Understanding Organic Reactions', Kluwer Academic, The Netherlands, 1989, pp. 33–53